**Electronic Supplementary Information**

for

# $^{17}$O solid-state NMR study on exposed facets of ZnO nanorods with different aspect ratio

Benteng Song,[*ac] Yuhong Li,[b] Yunhua Sun,[c] Luming Peng,[c] Ling-Hai Xie[*a]

[a] Key Laboratory for Organic Electronics and Information Displays (KLOEID) & Institute of Advanced Materials (IAM), Jiangsu National Synergetic Innovation Center for Advanced Materials (SICAM), Nanjing University of Posts & Telecommunications, 9 Wenyuan Road, Nanjing 210023, China

[b] Suzhou Key Laboratory of Functional Ceramic Materials, School of Materials Engineering, Changshu Institute of Technology, Changshu 215500, Jiangsu Province, China

[c] Key Laboratory of Mesoscopic Chemistry of Ministry of Education and Collaborative Innovation Center of Chemistry for Life Sciences, School of Chemistry and Chemical Engineering, Nanjing University, Nanjing 210023, China

[*] Correspondence: 1345385561@qq.com; iamlhxie@njupt.edu.cn

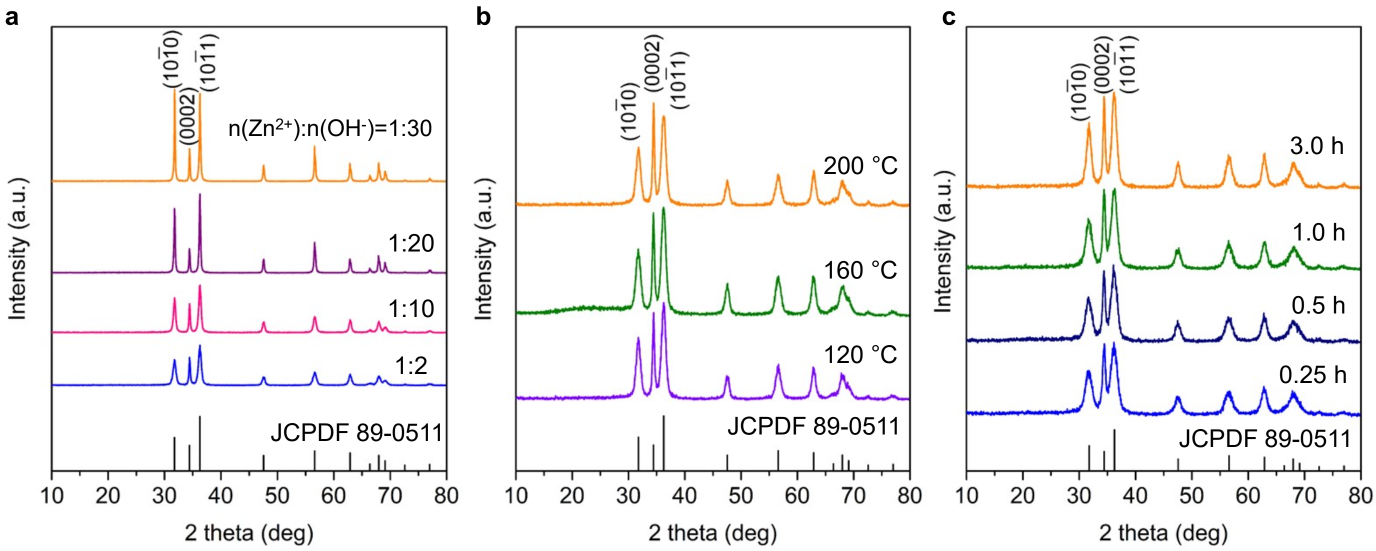


**Fig. S1** XRD patterns of ZnO nanorods prepared with different molar ratio of $Zn^{2+}/OH^-$ (a), hydrothermal temperature (b), and hydrothermal time (c).

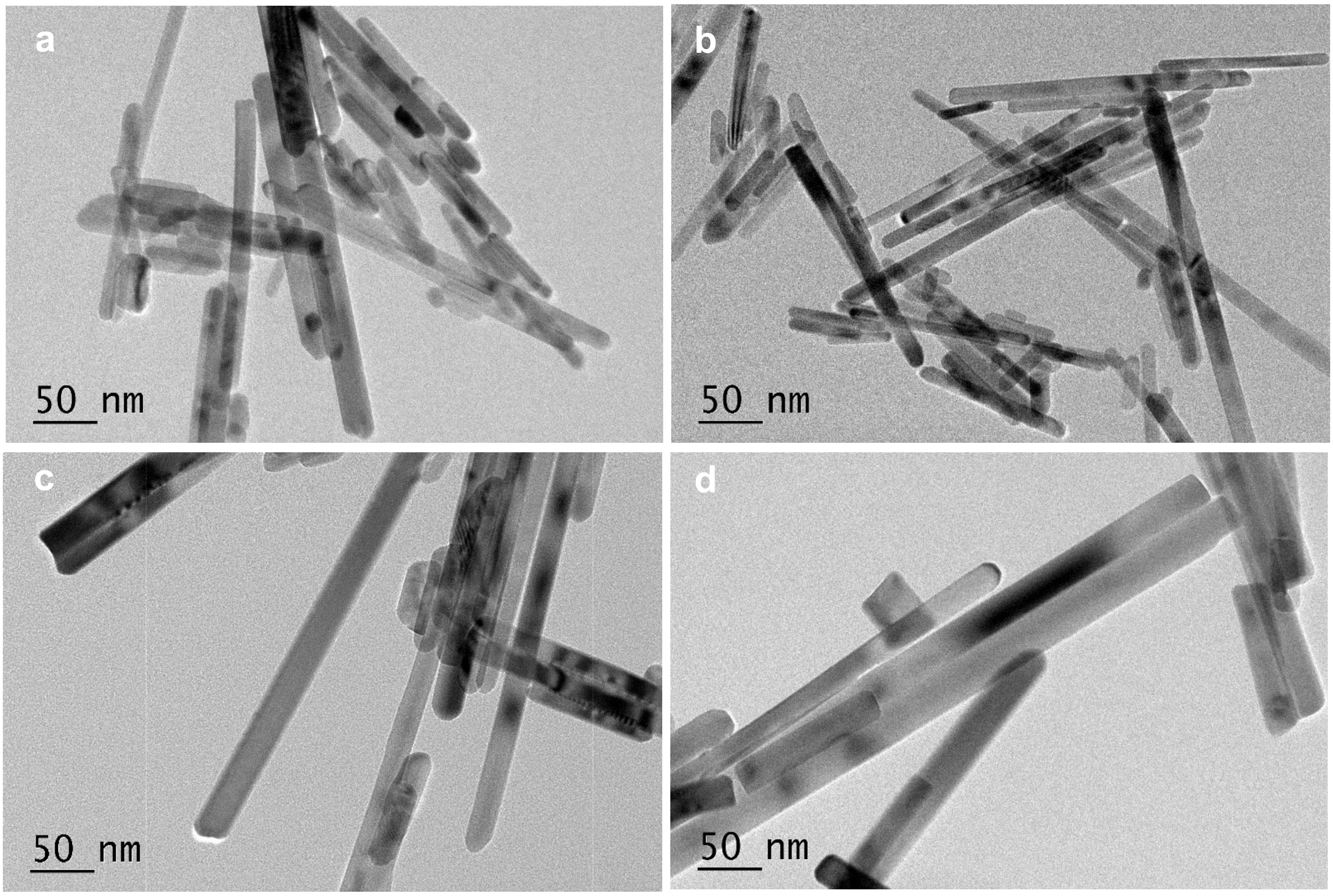


**Fig. S2** TEM images of ZnO nanorods with various molar ratios of $Zn^{2+}/OH^{-}$ (a-d: 1:2; 1:10; 1:20; 1:30). Data analysis on the length-to-diameter ratio can be found in Table S2.

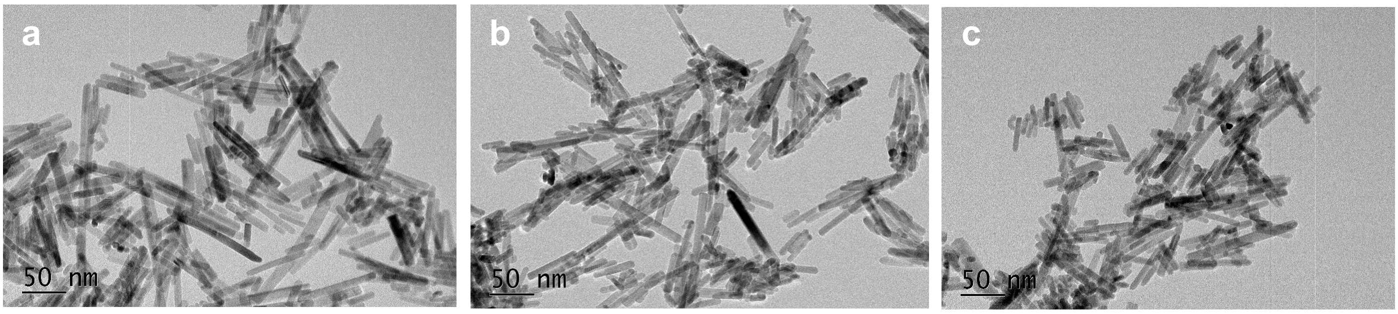


**Fig. S3** TEM images of ZnO nanorods with different hydrothermal synthesis temperatures (a: 120 °C, b: 160 °C, and c: 200 °C). Data analysis on the length-to-diameter ratio can be found in Table S2.

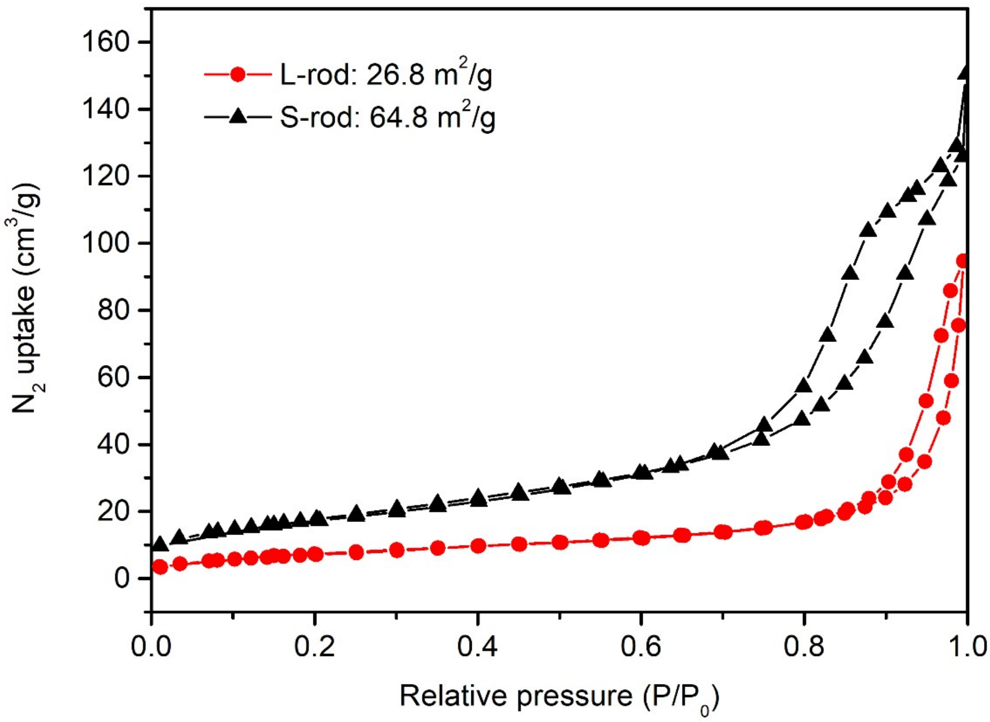


**Fig. S4** $N_2$ adsorption and desorption isotherms of L-rod and S-rod samples.

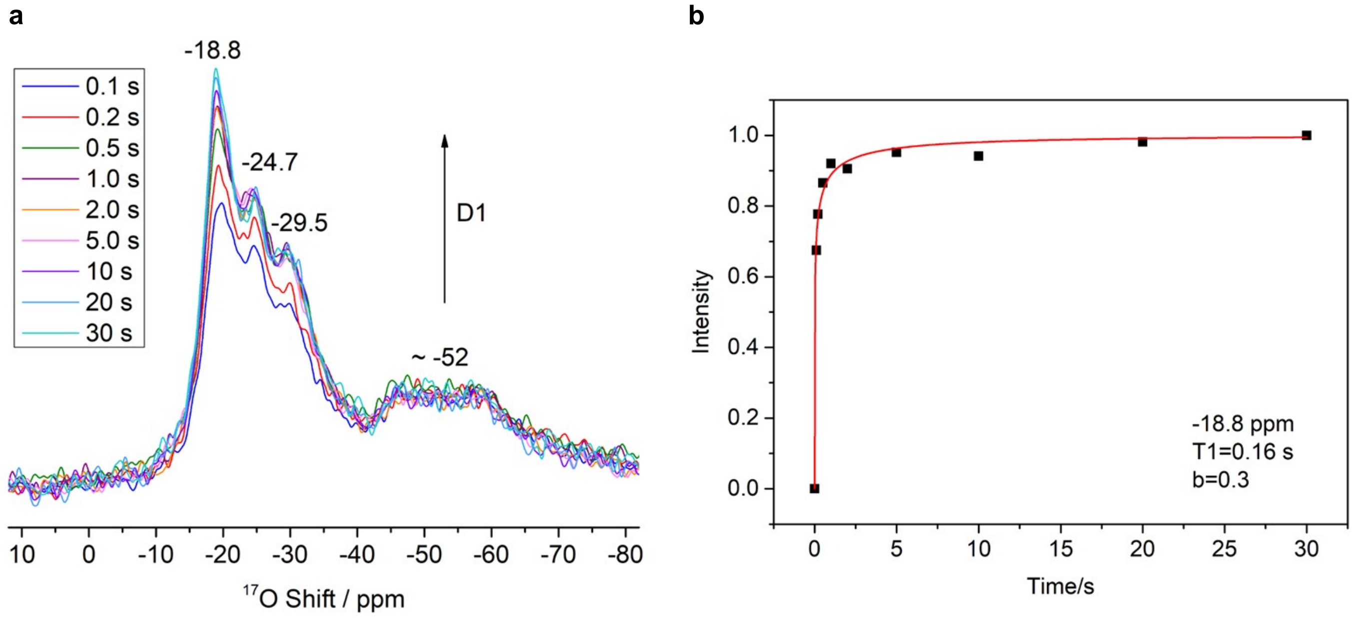


**Fig. S5** $^{17}$O MAS NMR spectra of L-rod. (a) $^{17}$O MAS NMR spectra of L-rod labeled with $H_2{}^{17}O$, as a function of the recycle delays from 0.1 to 30 s. The spectra were obtained at 9.4 T under a MAS frequency of 14 kHz. (b) $T_1$ analytical fit using a stretch exponential function of the type $I(\mathrm{t}) = I_0(1-e^{-(\frac{t}{T_1})^b})$, where $I$(t) and $I_0$ are the signal intensities at recycle delay $t$ and at equilibrium, respectively.

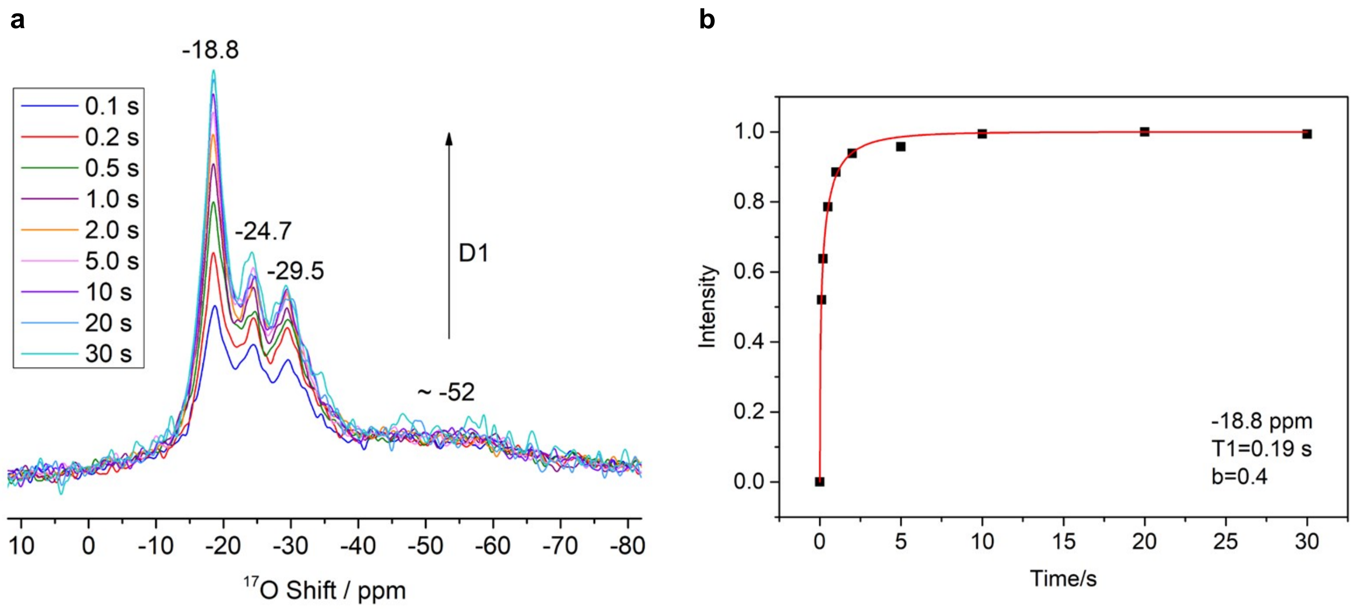


**Fig. S6** $^{17}O$ MAS NMR spectra of S-rod. (a) $^{17}O$ MAS NMR spectra of S-rod labeled with $H_2{}^{17}O$, as a function of the recycle delays from 0.1 to 30 s. The spectra were obtained at 9.4 T under a MAS frequency of 14 kHz. (b) $T_1$ analytical fit using a stretch exponential function of the type $I(t) = I_0(1 - e^{-(\frac{t}{T_1})^b})$, where $I$(t) and $I_0$ are the signal intensities at recycle delay $t$ and at equilibrium, respectively.

**Table S1** Data analysis on the length-to-diameter ratio of ZnO nanorods with different hydrothermal synthesis time.

| **Hydrothermal time/h** | **Diameter of (0002) facet/nm** | **Length/nm** | **Length/Diameter** | **Ratio of (100) facet/%** |
|---|---|---|---|---|
| 0.25 | 6 ~ 8 | 12 ~ 20 | 2.3 | 84.0 |
| 0.5 | 6 ~ 9 | 16 ~ 24 | 2.7 | 86.0 |
| 1.0 | 6 ~ 10 | 19 ~ 42 | 3.8 | 89.8 |
| 3.0 | 6 ~ 11 | 32 ~ 86 | 6.9 | 94.0 |

**Table S2** Data analysis on the length-to-diameter ratio of ZnO nanorods prepared as a function of the molar ratio of $Zn^{2+}/OH^{-}$ and hydrothermal temperature.

| **n($Zn^{2+}$):n($OH^{-}$)** | **Diameter of (0002) facet/nm** | **Length/nm** | **Length/Diameter** |
|---|---|---|---|
| 1:2 | 10 ~ 20 | 75 ~ 225 | 10 |
| 1:10 | 10 ~ 23 | 100 ~ 250 | 10.7 |
| 1:20 | 25 ~ 30 | 350 ~ 400 | 13 |
| 1:30 | 30 ~ 35 | 440 ~ 500 | 14 |
| **Hydrothermal temperature/°C** | **Diameter of (0002) facet/nm** | **Length/nm** | **Length/Diameter** |
| 120 | 7 ~ 12 | 49 ~ 157 | 11 |
| 160 | 7 ~ 9 | 47 ~ 98 | 9 |
| 200 | 6 ~ 8 | 38 ~ 69 | 7 |

**Table S3** NMR parameters including isotropic chemical shifts ($\delta_{iso}$) and quadrupolar parameters ($C_Q$ and $\eta$), used for simulating the $^{17}O$ NMR spectra in Fig. 4c, as well as simulated $\delta_{CG}$s for these species at 9.4 T.[1]

| $\delta_{iso}$ /ppm | $C_Q$ /MHz | $\eta$ | $\delta_{CG}$/ppm (9.4 T) | Assignment |
|---|---|---|---|---|
| -15.8 ± 0.4 | 1.19 ± 0.02 | 0.5 ± 0.5 | -18.9 | Surface $O_{3c}$ (M2) |
| -18.8 ± 0.2 | 0.10 ± 0.05 | 0.5 ± 0.5 | -18.8 | Subsurface $O_{4c}$ |
| -24.5 ± 0.15 | 0.40 ± 0.05 | 0.5 ± 0.5 | -24.8 | Surface $O_{4c}$ |
| -29.4 ± 0.2 | 0.30 ± 0.05 | 0.5 ± 0.5 | -29.6 | Surface $O_{4c}$ |
| -27.0 ± 1.5 | 1.75 ± 0.2 | 0.5 ± 0.5 | -33.7 | Surface $O_{3c}$ (M1D1) |
| -39 ± 1.5 | 2.50 ± 0.15 | 0.1 ± 0.1 | -52.0 | OH |

## References


1 B. T. Song, Y. H. Li, X.-P. Wu, F. Wang, M. Lin, Y. H. Sun, A.-P. Jia, X. Ning, L. Jin, X. K. Ke, Z. W. Yu, G. Yang, W. H. Hou, W. P. Ding, X.-Q. Gong and L. M. Peng, *J. Am. Chem. Soc.*, 2022, **144**, 23340–23351.